Sparse Range-Doppler Image Construction with Neural Networks

Jabran Akhtar
Norwegian Defence Research Establishment (FFI), Kjeller, Norway
Email: jabran.akhtar@ffi.no

***Abstract*—The principles outlined by compressed sensing can permit a sensor to collect reduced amount of data and still reconstruct an exact outcome. This can for example be used to generate super-resolution sparse range-Doppler radar images while emitting a reduced number of pulses within a coherent processing interval. In this paper, we investigate the use of neural networks as a mean to solve the sparse reconstruction problem with specific emphasis towards range-Doppler images. The neural networks are trained to generate a sparse Doppler profile from incomplete time domain data in line with traditional sparse L_1-norm minimization. We show that this approach is viable through fully connected feed forwarding networks and the results closely mimic sparse recovered range-Doppler maps.**

***Keywords*—Range-Doppler, discrete Fourier transform, compressed sensing, sparse reconstruction, neural networks**

I. Introduction

The usage of compressed sensing (CS) and sparse reconstruction (SR) techniques for various applications have been studied in great details over the last decade. These methods can permit a sensor, such as radar, to emit and receive fewer number of pulses while still being able to recover an exact result identical to as if all data was available [1], [2], [3], [4], [5], [6], [7], [8]. An important condition for this to succeed is the requirement of signal sparsity in some domain. Many type of radar setups can benefit from a CS approach where the overall environment may be considered to be sparse; for example when only a limited number of targets are likely to be present at a given range and/or angle.

A classical pulsed radar operating mode consists of the transmission of a number of pulses towards a set direction and the on-following generation of a range-Doppler map. In this process, each range bin is treated independently and the slow-time samples are Fourier transformed to yield a Doppler profile. Targets exhibiting a constant velocity emerge concentrated in Doppler and with each range bin containing a limited number of targets, the Doppler profile can be considered relative sparse. A radar employing CS techniques can thus implicitly introduce empty gaps within the data set and use sparse reconstruction methods to generate sparse range-Doppler maps. The empty gaps can instead be used to emit other type of radar pulses in alternative directions or frequencies. By assuming that additional gaps are located at the beginning and end of the pulse train the Doppler resolution can in principle be further enhanced [4], [9], [10], [11]. Multiple aspects of CS radars have been presented in previous works where the advantages and disadvantages have been discussed in details. One particular drawback of SR methods is that these algorithms are typically iterative and computationally demanding [12]. The number of iterations may also vary depending upon the exact data and is a source of unpredictable latency. This can make it difficult to implement such algorithms in systems with strict timing requirements.

Contiguous to CS, the usage and application of neural networks has gained significant hold over the years. Neural networks have been extensively employed for classification purposes, however, they have also shown strong adaptability towards other type of problems [13]. This work investigates the use of neural networks as a mean to solve the SR problem with emphasis on generation of range-Doppler maps. The objective of the neural networks will thus be to determine a sparse Doppler outcome from incomplete time domain data analogous to what a sparse recovery algorithm would have returned. This has been an unexplored area of research and opens up for new uses of neural networks in a radar context. The training for such a network is proposed carried out over a set of, specifically normalized, range-time profiles in conjunction with outcomes from an L_1-norm minimization procedure. We show that small fully connected feed forwarding neural networks can be trained to solve this type of problem and although the results are to a certain extent noise limited, and therefore not strictly sparse, they can nevertheless closely approximate sparse range-Doppler maps. The use of a neural network allows the reconstruction process to run in a determined time frame and may be implemented on dedicated neural or graphical processing units; making it a viable option to deploy sparse reconstruction techniques on practical setups. Some recent works have [14], [15] tried to link together compressed sensing and machine learning in other contexts, though a full complex output from a neural network inheriting a sparse recovered form of discrete Fourier transform (DFT) has not been presented before.

II. System design

A. Radar model and sparse recovery

In order to have a compressed sensing framework for the setup, we start by briefly reviewing the basic CS radar model [6], [11]; for more details on this section the cited references may be consulted. A pulsed radar is assumed where a waveform $p(t)$ is transmitted at regular intervals. The incoming echoes are sampled with a fixed rate and a matched-filtering operation is performed,

$$\mathbf{r}(t,u) = p^*(-t) * \ (\sum_n \sigma_n p(t-\Delta_n) e^{jv_{n,u}} + z(t)), \quad (1)$$

where $t = 1, 2, ..., R$. t is the discrete fast-time parameter corresponding to a time delay and therefore a range cell while R indirectly refers to the maximum radar range. N such pulses are transmitted in a coherent processing interval (CPI), $u = 1, ..., N$ (slow-time), and in the incoming target echoes σ_n and Δ_n point to, respectively, the reflectivity levels and the delay associated with reflector n. $j = \sqrt{-1}$ and $e^{jv_{n,u}}$ is

the Doppler shift for each target which for a constant velocity target is given by $v_{n,u} = v_{n,u-1} + \frac{\theta_n}{c}\frac{4\pi f_c}{\text{PRF}}$, assuming $v_{n,0} = 0$ and θ_n being the radial velocity of target n, PRF the pulse repetition frequency, f_c the radar carrier frequency and c the speed of propagation [16]. In (1), $*$ specifies convolution and $z(t)$ is white Gaussian noise. The targets are assumed to be slowly fluctuating and follow a Swerling one distribution where the values of σ_n vary from dwell to dwell with a given mean signal-to-noise ratio (SNR). After reception of all pulses the radar constructs a range-Doppler map; the slow-time domain of $\mathbf{r}(t,u)$ is multiplied with an arbitrary chosen window function $\mathbf{w}(u)$ and thereupon Fourier transformed, resulting in a range-Doppler representation:

$$\mathbf{D}(t,\omega) = \mathbf{F}\ \mathbf{w}(u)\ \mathbf{r}(t,u),\ \in \mathbb{C}^{N\times R}. \tag{2}$$

$\mathbf{F}$ is the discrete Fourier matrix of size $N \times N$, $\mathbf{F}_{k,l} = \exp(-j2\pi kl/N)$ while $\omega = 1, ..., N$.

In the proposed CS radar mode, it is assumed that the radar does not transmit N pulses immediately after each other rather the truncated range-time data matrix $\tilde{\mathbf{r}}(t,\tilde{u})$ only contains $M < N$ slow-time measurements, $\tilde{u} = 1, 2, ..., M$, collected arbitrary, or quasi-arbitrary, within the coherent interval of N pulses. With irregular and incomplete data, a traditional range-Doppler map will show targets spreading out exceedingly in Doppler with a reduced peak SNR. A sparse reconstruction solution should thus interpolate the gaps, and possibly extrapolate at the edges, to generate a solution in Doppler domain where the targets have been refocused. For this we define L to indicate the number of desired output entries in Doppler and assume that $L \geq N$; an $L > N$ signifying extrapolation in slow-time. For a fixed range bin $T = 1, ..., R$, the reconstruction problem under convex relaxation can be described as [11]

$$\hat{\mathbf{D}}(T,\hat{\omega}) = \arg\min_{\dot{\mathbf{D}}} ||\dot{\mathbf{D}}(T,\hat{\omega})||_1 \tag{3}$$

subject to

$$||\ \hat{\mathbf{F}}_R\ \dot{\mathbf{D}}(T,\hat{\omega}) - \bar{\mathbf{w}}(\tilde{u})\ \tilde{\mathbf{r}}(T,\tilde{u})\ ||_2 \leq \varepsilon_T \tag{4}$$

where ε_T is acceptable error limit and $\hat{\omega} = 1, ..., L$ indicates the Doppler bins. $\hat{\mathbf{F}}_R \in \mathbb{C}^{M\times L}$ is the partial inverse Fourier matrix constructed from an $L \times L$ matrix where rows corresponding to gaps in time positions have been removed. Similarly, $\bar{\mathbf{w}}(\tilde{u})$ is a truncated windowing function of M entries, from an original length of L, with $\max_{\tilde{u}} \bar{\mathbf{w}}(\tilde{u}) \leq 1$.

The reconstructed Doppler profile must maximize sparsity which is achieved if objects of interest are projected with a determined velocity and thus become more narrowly confined. Finding an independent solution over all range bins results in a range-Doppler map matrix $\hat{\mathbf{D}}(t,\hat{\omega})$ where any missing data would effectively have been inter- or extrapolated. Omitting the indexes, the recovery process may also be specified as a function on the form $\hat{\mathbf{d}} = f_{SR}\ (\tilde{\mathbf{r}}),\quad \mathbb{C}^M \rightarrow \mathbb{C}^L$ where $\hat{\mathbf{d}} = \hat{\mathbf{D}}(T,\hat{\omega})$ for a fixed T.

As already pointed out, one can infer that the data beyond the CPI sampling intervals is also missing. Time domain data at the edges is often heavily weighted down by tapering functions before a Fourier transform and an extrapolation on both ends can therefore aid in improving data utilization. The process is illustrated in figure 1 where 0 indicates a position with no

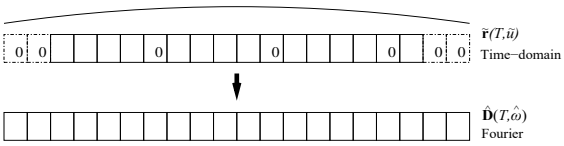

Fig. 1: Sparse reconstruction with extrapolation

acquired data. By determining an independent L_1 solution over a number of signal realizations, a training set can accordingly be founded where each, normalized and tapered, time-range profile, with possible gaps, is mapped into a Doppler profile obtained through sparse reconstruction.

B. Sparse reconstruction with neural networks

The main objective of a trained neural network should be to approximate the f_{SR} function. A successful outcome is thus strongly dependent on the network's ability to learn and execute a type of DFT. To perform the neural network training we assume that a large number of varying signal realizations over various CPIs have been gathered, i.e. the inputs and outputs of f_{SR}. The main parameters N, M and L are expected to be known and fixed and the gaps are also to remain at the same position for a given data set which otherwise satisfies the requirements for spare reconstruction. For each realization, $\tilde{\mathbf{r}}(T,\tilde{u})$, normalized by ρ_T (as defined later) and the Doppler profile output from the sparse reconstruction process, $\hat{\mathbf{D}}(T,\hat{\omega})$, is presumed to have been computed and thus readily available (figure 1). More specifically, the training database is constructed on the input and outputs of $\hat{\mathbf{d}} = f_{SR}(\tilde{\mathbf{r}}/\rho_T)$.

To deal with complex input and output values we split the data in two, a real and an imaginary part and feed them into the neural network as separate entities. Since the gaps (including extrapolation gaps) do not shift locations they can be eliminated from the input stream. The $2M$ inputs to the neural networks are normalized by dividing them by the maximum absolute value, i.e.

$$\rho_T = \max\left(|\Re(\tilde{\mathbf{r}})|,\ |\Im(\tilde{\mathbf{r}})|\right). \tag{5}$$

The largest absolute value for each input will thus equal one while the lowest figure remains undefined. It turns out that this normalization plays a key role for successful training of the network. Other normalization techniques such as min-max or z-score tend to compress the dynamic range of the data and do not lead to successful outcomes. As the DFT is a linear process, a multiplication by ρ_T is to be transacted at the other end to denormalize but this aspect is retained outside the neural network and the training procedure. It can be shown that a single hidden layer is sufficient to make a neural network perform a DFT. For this extended concept, we propose to use classical fully connected feed forwarding neural networks with at least the same number of nodes in each layer as the number of inputs and at least two hidden layers. Each node utilizing the $tanh$ activation function. The $2L$ outputs from the final layer are combined at the end to form half as many complex digits. Figure 2 gives a visual depiction the neural network design.

To obtain network convergence close to sparse recovery results, a large set of example data is necessary that should span much of the Doppler space in addition to targets with

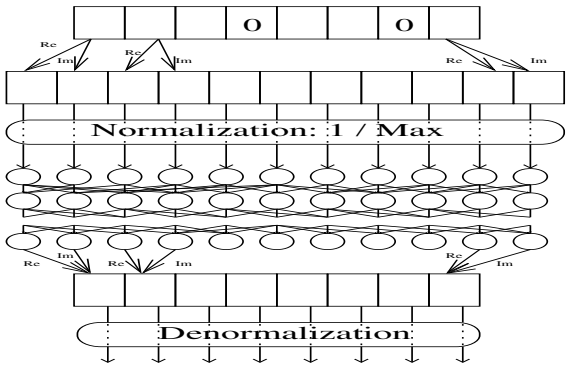

Fig. 2: Neural network process

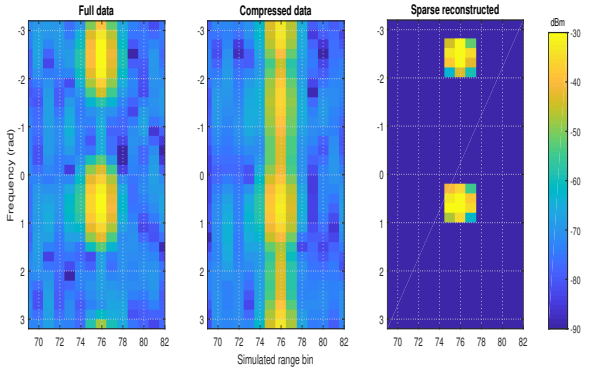

Fig. 3: Example of range-Doppler map data used for training

variable magnitudes. This can be achieved if a set of range-Doppler maps is available where a target, or multiple targets, are localized at different velocities with alternating power levels. This must come in addition to noise only profiles yielding an all empty response from sparse reconstruction.

One particular aspect to be aware of is that the output solution from an L_1 optimization problem will contain values exactly equal to zero. This is probably difficult for a conventional neural network to duplicate where the final nodes are more likely to return small noise-like figures instead of strictly zero. These values may therefore tend to further inflate when denormalized.

III. Training Examples

With the above remarks in mind, a radar environment consisting of targets placed at different ranges was simulated. The pulsed radar processed $N = 16$ pulses within a dwell and the targets followed a standard Swerling one model where the mean varied randomly from CPI to CPI to mirror different power levels. The targets were further assumed to have two sidelobes in range on both sides of -20dB and -26dB and the target velocity was randomly selected for each CPI. The noise floor was likewise randomly changed and varied between -100dB to -110dB following a uniform distribution between CPIs. The PRF was simulated at 3kHz with a carrier frequency of 3GHz and the Blackman window was put to use for all Doppler processing.

A neural network training can occur assuming a range bin contains either only noise or a single target with noise, however, this will also imply that the network may not adapt well to the case of multiple targets. This is not necessarily a problem as sparse reconstruction also requires that the signal to be recovered should be sparse. Nevertheless, in order to train the neural network for a slightly more generic case, we model a particular range bin to contain up to two potential targets with two randomly selected velocities. With a probability of 50%, each of these two targets are to follow independent Swerling one power distribution while for the remaining half the targets have identical intensity values. If each of the target adhere to independent fading at all times, then in a large number of cases, one of the targets will be stronger then the other one and overpower the weaker target in the optimization process. It was found that this is alleviated by making sure that both of the targets have equal magnitude for a number of realizations.

A total of 30000 such range-time data constructions were generated and in the subsequent range-Doppler maps the target SNR ended up varying between -40dB and 85dB. To construct the training database, range bin containing the target and the sidelobes were extracted in addition to a single range bin containing noise only. This gives a total of 4 range-time, $\mathbf{r}(t,u)$, profiles per CPI leading to a total of 120000 training specimens. For all of these samples, two compressed sensing data collection strategies were selected. The first one consisted of three gaps ($M = 13$) placed in slow-time at positions 4, 9 and 11. The second setting increased the number of gaps to six ($M = 10$). The time domain data was accordingly maximum absolute normalized, $\tilde{\mathbf{r}}(T,\tilde{u})/\rho_T$, and a sparse recovery procedure was performed under the criteria $\varepsilon_T < 1 \cdot 10^{-3}/\rho_T$ for each T or bin. In the recovery operation, 8 extrapolations on both ends were incorporated resulting in an output of $L = 32$ Doppler bins per range bin, corresponding to 64 output values from the neural network. Fully connected feed forwarding neural networks of different sizes were considered in this work; a single layer network of 64 nodes, a network with two hidden layers each containing 64 nodes, a deeper network with 6 hidden layers and 64 nodes in each layer and a wider type of network with 192 nodes in two hidden layers. A small network is generally easier to train and less computationally demanding while bigger networks may approximate the data better but may be more prone to overfitting. The training of the defined networks was executed for up to a million epochs.

A. $N = 16, M = 13, L = 32$

An example of parts of such a randomly generated range-Doppler map used for training is provided in figure 3. The left image, for reference, represents the standard range-Doppler map assuming all data is available. The middle image shows the outcome with incomplete data where traditional Doppler processing has been applied assuming the empty gaps are set to zero values. As expected, the target spreads out in frequency and suffers SNR loss. The sparse recovery results executed on gapped data are given in the figure on the right side. Sparse reconstruction refocuses the targets while the introduction of time domain extrapolation aids in amending the Doppler resolution. The maximum absolute normalized range-time version of the middle image would constitute the input for training while the normalized image on the right the output.

To assess the results from the trained neural networks, a series of evaluation signals were generated over $t = 1, ..., 800$

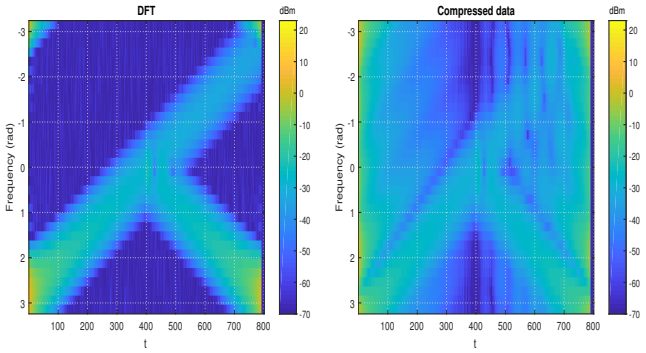

(a) Full data (b) Incomplete data ($M = 13$)

Fig. 4: Reference range-Doppler maps

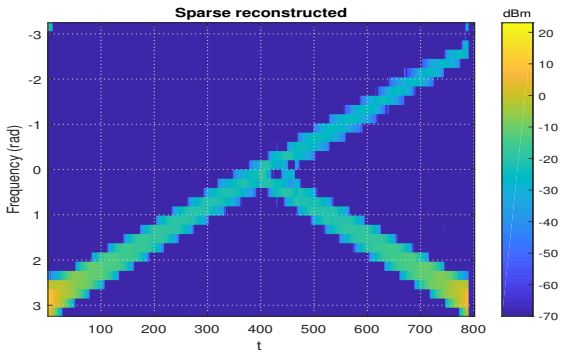

Fig. 5: Sparse reconstruction ($M = 13, L = 32$)

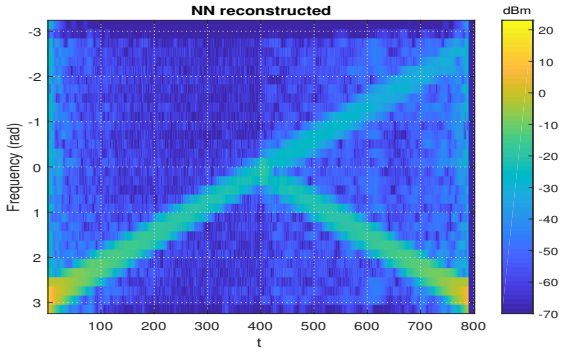

Fig. 6: NN (64×2) reconstruction ($M = 13, L = 32$)

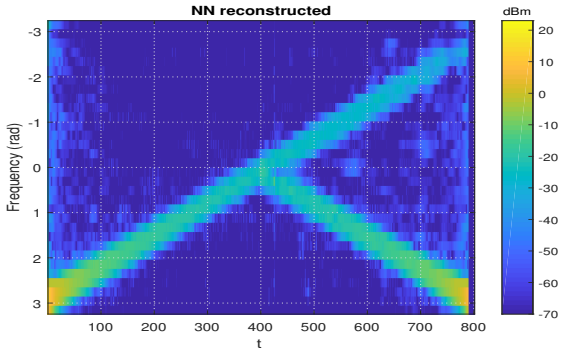

Fig. 7: NN (192×2) reconstruction ($M = 13, L = 32$)

simulated range bins. A single target was incorporated in each bin with a sweeping velocity over t with the objective to cover the full frequency range. The target power was additionally set to decrease gradually as t increased. For the second half of the bins, a second target was introduced with increasingly power level and a sweeping velocity in the opposite direction. To also evaluate the performance in noise only situations the last ten range bins were free of any targets and the noise level in slow-time data was at -70dBm.

The left side image in figure 4 depicts the range-Doppler map with all available data while the right side shows the result in case of gapped data. The sparse recovery process on incomplete data, with $L = 32$, returns figure 5 where the targets are easily identifiable and highly concentrated in Doppler for all velocities and intensities. This sparse image establishes a reference point for what a neural network should aim for.

Feeding the identical incomplete time domain data to the trained neural networks (NN) results in the two images shown in figure 6 for the case of the smaller 64×2 network and figure 7 for the wider 192×2 neural network. Both networks are able to identify the main features and localize the targets who clearly stand out. The primary process behind transforming data from slow-time to DFT is hence in place. The reconstruction, particularly with the smaller network, is obviously not sparse rather a noise floor is evident. The right region of the image, with two targets, is noisier and more granular which can be attributed to the fact that there is more energy present which the network is not able to fully suppress. The wider network though succeeds much better in reducing the noise floor to around -70dBm which is very close to the original noise floor level though inflated noise can still be observed at range bins with energetic targets. The extreme right range bins, without any active targets, exhibit a noise floor of -120dBm for 64×2 network and -131dBm for 192×2 network.

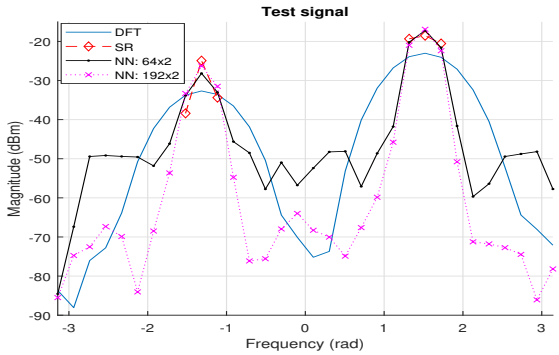

Fig. 8: Signal extraction at range bin 600

To provide further insight, figure 8 details the Doppler profiles for $t = 600$ from the maps. The blue curve portrays the full data DFT response while the red line characterizes the sparse recovery results from incomplete data which retrieves three non-zero values for each peak. As already pointed out, a neural network can not yield exactly zero outcomes, however, for the case of the bigger network (dotted magenta), the non-peak values are relative small and either comparable to the DFT or improve on that. The smaller 64×2 network (black)

also approximates the maxima very well but the noise floor is more prominent. Both networks manage to improve the peak SNR and narrow down the target localization reciprocating sparse recovery reconstruction.

Network size	Performance error on training data	Relative error on evaluation image, μ	Dynamic range (dB)
64x1	0.2580	0.2758	138.23
64x2	0.1040	0.1919	141.75
64x6	0.0617	0.1976	144.75
192x2	0.0411	0.1875	156.15

TABLE I: Neural network performance ($M = 13, L = 32$)

To quantify these results, table I gives numerical error values where the outcomes from the various sized networks are compared against the sparse recovery results. The performance error, on the leftmost column, is defined as the norm error between the factual and desired network output on training data at the end of the optimization session. These error rates are generally low and decrease as the network size increases. The relative norm error, in the third column, is the error between the evaluation image formed by the sparse reconstruction process W_{SR} and the neural network output, W_{NN}, where each range bin is normalized to the peak value of 1, defined as $\mu = ||W_{NN} - W_{SR}||_2/||W_{SR}||_2$. The discrepancy in this across the networks is rather small implying that the main features are approximated just as well regardless network size. The last column of the table gives the dynamic range of the image, i.e. the difference between the maximum and the smallest value, excluding the rightmost range bins. For reference, the dynamic range in the original complete data image is at 146.01dB. The wider network is able to yield a much better result which is also very visible. It is noteworthy that a deep network (64×6) only provides marginal improvement over a 64×2 network while increasing the width, with more nodes in each layer, offers a much more profound impact on the performance. If the nodes need all available input data to compute the output, which is indeed the case with a DFT, then this is favorably attainable with a wider network.

B. $N = 16, M = 10, L = 32$

To verify that the neural networks are adaptable also for more demanding scenarios, the same type of sparse recovery and optimization process was executed with the second CS data collection strategy leading to a further reduction in gathered data. Six pulse gaps were therefore introduced at dwell positions 2, 4, 9, 11, 14 and 15; with acceptable performance, this would imply that a radar could operate with a limited set of only $M = 10$ emitting pulses without noticeable degradation as compared to a radar emitting 16 pulses. The evaluation image was otherwise kept identical to the previous case. The left side image in figure 9 shows the compressed data range-Doppler map while the right side demonstrates the result with sparse reconstruction. The sparse outcome is still of very high quality and can distinguish the two targets easily. The outcomes from the trained neural network are given in figure 10 where the images, like preceding cases, are not fully sparse though the level of noise is on par with earlier results. Importantly, the trained networks manage to identify and separate the two targets adequately. A numerical evaluation is given in table II. Comparing table II to table I, having a greater number of gaps slightly increases the error rates and reduces the dynamic range by 2-3dB though still augmenting the standard complete data range-Doppler map.

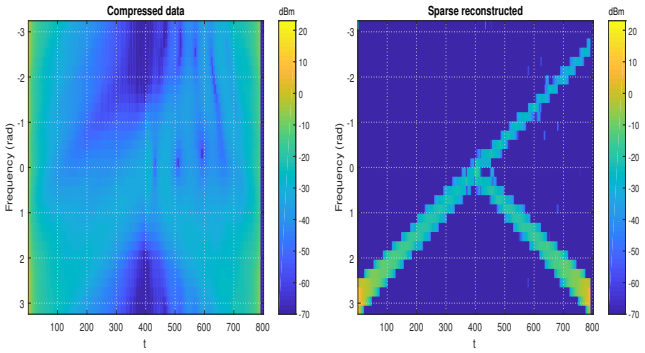

(a) Incomplete data (b) Sparse reconstruction

Fig. 9: Range-Doppler maps ($M = 10, L = 32$)

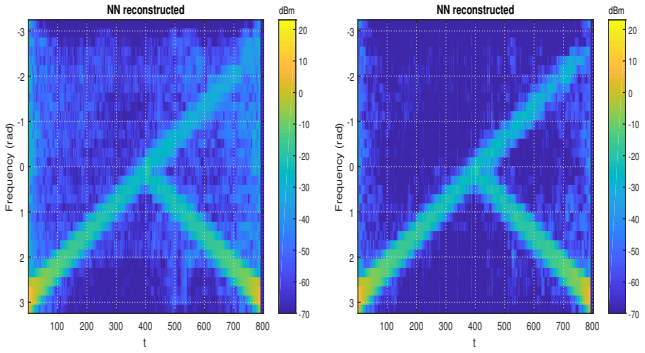

(a) 64×2 (b) 192×2

Fig. 10: NN reconstruction ($M = 10, L = 32$)

C. Additional targets

The neural networks above have been all been trained on the presumption of up to two potential targets in a given range bin. Sparse reconstruction also places bounds on the required sparsity level for perfect recovery, nevertheless, it can be interesting to examine how the networks react if additional targets are introduced even though no explicit training for this has been carried out. A different set of simulated signals were therefore generated over the simulated range bins. Two sweeping targets were introduced with increasing/decreasing power and an additional third one with a fixed zero Doppler and incriminating return. The left image in figure 11 depicts the standard gapped range-Doppler map with $M = 13$ while the right image demonstrates the use of sparse recovery on this scenario. The recovery process manages to bring forth all three targets albeit the reconstruction is not fully sparse with certain combinations causing velocity ambiguities.

The neural network results, from the previously trained networks for $M = 13$, are given in figure 12. Notice that

Network size	Performance error on training data	Relative error on evaluation image, μ	Dynamic range (dB)
64x2	0.1420	0.2490	136.74
192x2	0.0574	0.2165	153.50

TABLE II: Neural network performance ($M = 10, L = 32$)

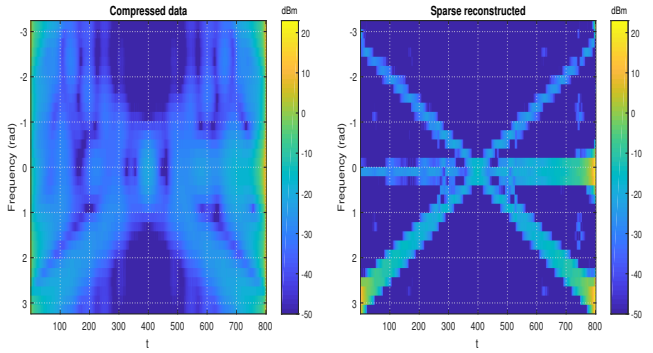

(a) Incomplete data (b) Sparse reconstruction

Fig. 11: Range-Doppler maps ($M = 13, L = 32$)

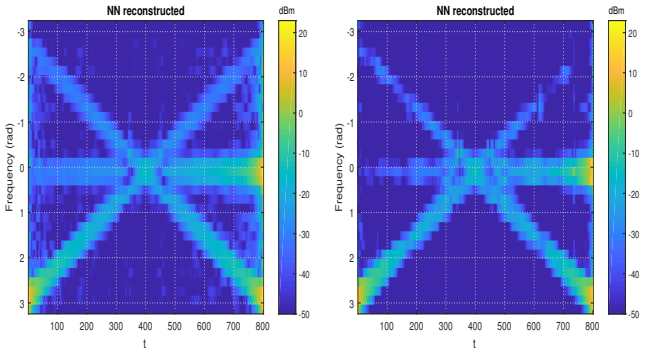

(a) 64×2 (b) 192×2

Fig. 12: NN reconstruction ($M = 13, L = 32$)

the lower axis bound is now set at -50dBm to overlook the noise floor. It is particularly with the smaller network, on the left, where all three targets clearly stand out and are easy to identify. The wider network (right image) is more favorable with respect to noise reduction but does not manage to resolve the weaker targets. This network has presumably specialized itself a greater extend to identify only up to two targets and does not develop as well under different circumstances.

This does demonstrate that the networks have not simply memorized the different cases but are performing a more generic process to evaluate Doppler profiles from gapped data. A neural network can thus be trained to generate range-Doppler maps and to some extent replace the sparse recovery process in data collected through compressed sensing approaches subject to a perceptible noise floor. To obtain fully sparse profiles, one may operate with a threshold limit on the output from the final nodes or alternatively other type of neural network designs could be implemented.

IV. Conclusion

Compressed sensing allows a pulsed radar to introduce gaps in slow-time data and utilize sparse recovery to reconstruct high resolution range-Doppler maps. A generic framework on how this recovery process can be trained and implemented via neural networks was presented. The training for such a network was carried out over maximum absolute normalized versions of range-time profiles containing fluctuating targets and noise. The desired output was determined by a sparse recovery procedure. The results show that a fully connected neural network can indeed learn to return Fourier profiles from incomplete slow-time data and thus function as a replacement for sparse recovery algorithms. The output from smaller neural networks tend to have a low dynamic range though this can be mitigated by employing wider networks. This makes it viable to execute the sparse reconstruction process in a fixed time frame without relying on computational algorithms.

References

[1] E. Candès, J. Romberg, and T. Tao, "Stable signal receovery from incomplete and inaccurate measurments," *Communication in Pure and Applied Mathematics*, vol. 59, pp. 1207–1223, 2006.

[2] L. C. Potter, E. Ertin, J. T. Parker, and M. Cetin, "Sparsity and compressed sensing in radar imaging," *Proceedings of the IEEE*, vol. 98, no. 6, pp. 1006–1020, 2010.

[3] M. F. Durate and Y. C. Eldar, "Structured compressed sensing: From theory to applications," *IEEE Transactions on Signal Processing*, vol. 59, pp. 4053–4085, 2011.

[4] M. A. Herman and T. Strohmer, "High-resolution radar via compressed sensing," *IEEE Trans. Signal Processing*, vol. 57, no. 6, pp. 2275–2284, June 2009.

[5] K. Mishra, M. Cho, A. Kruger, and W. Xu, "Off-the-grid spectral compressed sensing with prior information," in *IEEE International Conference on Acoustics, Speech and Signal Processing*, 2014, pp. 1010–1014.

[6] J. Akhtar and K. E. Olsen, "A compressed sensing based design for formation of range-Doppler maps," in *Proc. of IEEE Radar Conference*, 2016, pp. 35–39.

[7] D. Cohen and Y. C. Eldar, "Reduced time-on-target in pulse Doppler radar: Slow time domain compressed sensing," in *Proc. of IEEE Radar Conference*, 2016.

[8] P. Addabbo, A. Aubry, A. D. Maio, L. Pallotta, and S. L. Ullo, "HRR profile estimation using SLIM," *IET Radar, Sonar & Navigation*, vol. 13, no. 3, pp. 512–521, April 2019.

[9] J. Yang, J. Wright, T. S. Huang, and Y. Ma, "Image super-resolution via sparse representation," *IEEE Trans. Image Processing*, vol. 19, no. 11, pp. 2861–2873, Nov. 2010.

[10] L. Anitori, W. van Rossum, and A. Huizing, "Array aperture extrapolation using sparse reconstruction," in *IEEE Radar Conference*, 2015, pp. 237–242.

[11] J. Akhtar and K. E. Olsen, "Formation of range-Doppler maps based on sparse reconstruction," *IEEE Sensors Journal*, vol. 16, no. 15, pp. 5921–5926, Aug. 2016.

[12] E. C. Marques, N. Maciel, L. A. Naviner, H. Cai, and J. Yang, "A review of sparse recovery algorithms," *IEEE Access*, vol. 7, pp. 1300–1322, Dec. 2018.

[13] H. Huttunen, *"Deep neural networks: A signal processing perspective"*. Handbook of Signal Processing Systems (Third Edition), S. S. Bhattacharyya, E. F. Deprettere, R. Leupers, and J. Takala, Eds. Springer, 2019.

[14] C.-H. Z. and; Y.-L. Xu, "An improved compressed sensing reconstruction algorithm based on artificial neural network," in *International Conference on Electronics, Communications and Control*, 2011, pp. 1860–1863.

[15] M. Mardani, E. Gong, J. Cheng, S. Vasanawala, G. Zaharchuk, L. Xing, and J. Pauly, "Deep generative adversarial neural networks for compressive sensing MRI," *IEEE Transactions on Medical Imaging*, vol. 38, no. 1, pp. 167–179, Jan. 2019.

[16] W. L. Melvin and J. A. S. (Eds.), *Principles of Modern Radar*. SciTech Publishing, 2013.